Effects of electron-electron interactions on the valence-band photoemission spectra of metals*

Steven Prutzer† and Shyamalendu M. Bose
Department of Physics and Atmospheric Science, Drexel University, Philadelphia, Pennsylvania 19104
(Received 9 April 1984)

The effects of secondary electron-hole pair production on the valence-band x-ray photoemission spectra of metals have been investigated. In the first-order theory, the intensity in the main band diverges due to the production of very weak energy electron-hole pairs. Hole renormalization is therefore included to study the intrinsic, inelastic process in the main band region, the quantum interference between the intrinsic and extrinsic processes, and the tailing of the main band due to elastic hole scatterings. The resulting spectrum is found to be smooth and finite over the entire spectral range. The calculated spectrum for sodium extending from the main band to the tail of the first bulk-plasmon satellite is compared with presently available experimental data.

I. INTRODUCTION

The core-level x-ray photoemission spectroscopy (XPS) of simple metals has been under investigation for some time.[1–24] The dominant physical effects which give rise to the asymmetry of the main line have been studied by several authors.[2–4] The satellites due to bulk- and surface-plasmon productions and the background intensity due to single-particle excitations have also been studied both theoretically[3–12] and experimentally.[13–24]

In comparison with the level of activity on the core-level spectra, the valence-band photoemission spectra of metals have remained relatively unnoticed.[21–30] In two previous publications with Longe,[29,30] we reported on the strength and shape of the first bulk-plasmon satellite in the valence-band photoemission spectra of simple metals. In this paper we consider the effects of single, secondary electron-hole pair creation on the valence-band photoemission spectra of metals, with the expectation that it will alter the shape and strength of the main band and introduce tailing in the lower-energy region, thereby explaining the experimentally observed spectra.[21–25]

As in the case of core-level XPS, we consider the intrinsic processes due to the interaction of the primary hole in the conduction band with the surrounding electron gas, the extrinsic pair productions by the photoelectron, and the quantum interference between these two processes. As with the plasmon satellite case,[29,30] we expect that the mobility of the primary hole in the conduction band will have a significant effect on the calculated spectra, and hence we will keep the recoil of this hole in the present calculations. Calculations in this paper are carried out using the S- and T-matrix formalism which was recently introduced by Longe and co-workers,[4,9] to study the core-level photoemission spectra of simple metals.

In Sec. II we present our model of the valence-band XPS in detail and show, in general, how these results relate to those of Ref. 30. In Sec. III we present our calculation and results, and in Sec. IV we shall summarize and draw our conclusions.

II. FORMALISM

Our calculations are made for the jellium model of a metal filling the half plane $z>0$ at temperature $T=0$. For emission of photoelectrons normal to the surface, the intensity of photoemission to order n in the effective Coulomb interaction can be written as

$$I_n(\varepsilon_k)=\int_0^\infty d\tau\, V_k J_n(\varepsilon_k,\tau)\ . \tag{1}$$

V_k is the speed of the photoelectron of wave number k in the metal, τ is the transit time from the site of ionization to the surface, and $J_n(\varepsilon_k,\tau)$ is the probability of an electron leaving the metal after an nth-order process (plasmon production or single-particle excitation). Equation (1) assumes a constant density of primary ionization (equal to 1) in the metal. $J_n(\varepsilon_k,\tau)$ can be written in terms of a τ-dependent S-matrix element by using the time-dependent golden rule. We express these matrix elements as diagrams which are shown, for orders 0 and 1 in the effective Coulomb interaction, in Fig. 1. As in Ref. 30, bare propagators are used for the valence hole line (pointing downward) and the electron line (pointing upward). The wavy lines entering the lower vertices in Fig. 1 represent the incoming x-ray photon, and the dashed lines represent the interactions with the surrounding system of electrons in the metal. For these interactions we use the random-phase approximation (RPA) of the effective Coulomb interaction, $\mathscr{V}(q,\omega)$, defined by

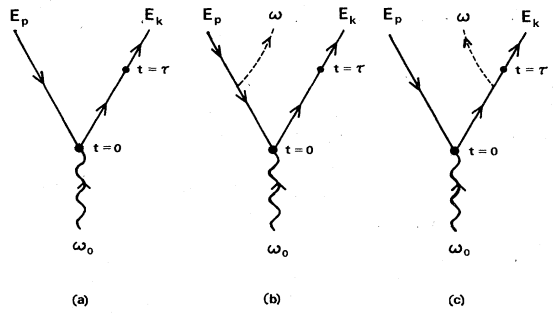

FIG. 1. Diagrams representing the x-ray photoemission process to (a) order 0, and (b) and (c) order 1 in the effective Coulomb interaction (dashed lines). The photoelectron line, pointing upward, can have no interactions with the bulk after time τ, when it leaves the metal.

$$\mathscr{V}(q,\omega)=v(q)-v(q)B(q,\omega)\mathscr{V}(q,\omega)=\frac{v(q)}{\epsilon(q,\omega)} . \quad (2)$$

In Eq. (2), $v(q)$ is the bare Coulomb interaction, $B(q,\omega)$ is the lowest-order polarization propagator, or "bubble" diagram, and $\epsilon(q,\omega)$ is the dielectric function in the RPA.

Since XPS involves a photoelectron leaving the system and being detected, conservation of energy between the initial and the final states will hold. This means that the secondary electron-hole pairs of the effective interaction, as shown in Fig. 1, exist as real pairs in the final state. For this reason it is only necessary to consider $\mathscr{V}(q,\omega)$ for $\omega \geq 0$, represented by $\mathscr{V}_+(q,\omega)$.

As in the case of soft x-ray emission spectra[31] and Auger emission spectra of simple metals,[32] we will find that this first-order theory yields unphysical results. Problems occur at the low-energy end of the main band of the spectrum, in the zeroth-order and interference terms, and throughout the main band for the intrinsic term.[33] This is due to the neglect of finite lifetime effects for the primary hole, excited in the valence band by the incident photon. As we will see in Sec. II B, these effects can be taken into account by appropriate renormalization of the primary hole.

A. Without hole renormalization

As in previous calculations with Longe *et al.*[4,9,29,30] we find a τ-dependent exponential term in the photoelectron propagator and are able to write $J_n(\varepsilon_k,\tau)$ in terms of the T-matrix elements. This is equivalent to closing the diagrams of Fig. 1. $J_n(\varepsilon_k,\tau)$ is then written as

$$J_n(\varepsilon_k,\tau)=\frac{(4\pi k_F^3/3)^{-1}}{Nn!}\int d\omega \int d^3p\,\Theta(k_F-p)\delta(\varepsilon_k+n\omega-\varepsilon_p-\omega_0)\times\begin{cases}\delta(\omega), & n=0\\ T(\varepsilon_k,\varepsilon_p,\tau,\omega), & n=1\end{cases} \quad (3)$$

with

$$T(\varepsilon_k,\varepsilon_p,\tau,\omega)=\frac{1}{(2\pi)^3}\int d^3q\left[\frac{-\mathrm{Im}\mathscr{V}_+(q,\omega)}{\pi}\right]\left|\frac{\Theta(k_F-|\vec{p}-\vec{q}|)}{\mu(\vec{p},\vec{q},\omega)}-\frac{1-e^{i\nu(\vec{k},\vec{q},\omega)\tau}}{\nu(\vec{k},\vec{q},\omega)}\right|^2 . \quad (4)$$

The hole propagator in Eq. (4) is $\mu^{-1}=(\omega+\varepsilon_{|\vec{p}-\vec{q}|}-\varepsilon_p+i\lambda)^{-1}$, and $\nu^{-1}=(\omega+\varepsilon_k-\varepsilon_{|\vec{k}+\vec{q}|})^{-1}$ is the propagator for the photoelectron (note that the following identification is made throughout this paper: $\varepsilon_p=p^2/2m$, $\hbar=1$); Θ is the step function, ω_0 the incoming photon energy, and λ a positive infinitesimal. Note that $\mathrm{Im}\mathscr{V}_+(q,\omega)$ is nonzero only when $\omega>0$. The plasmon-pole part of $\mathrm{Im}\mathscr{V}_+(q,\omega)$ and the single-particle excitation part occur for distinct values of (q,ω). The single-particle portion, only, is used in our present calculations, and will be referred to as $\mathrm{Im}\mathscr{V}_+^{\mathrm{sp}}(q,\omega)$. Similarly I, J, and T will be referred to as I^{sp}, J^{sp}, and T^{sp}. N^{-1} is the normalization factor which gives conservation of probability when all order processes are considered and has been discussed in detail in a previous article.[4] The form of N^{-1} is taken to be

$$N^{-1}=\exp\left[-(4\pi k_F^3/3)^{-1}\int d^3p\,\Theta(k_F-p)\int d\omega\, T^*(\varepsilon_k,\varepsilon_p,\tau,\omega)\right] . \quad (5)$$

The asterisks in Eq.(5) and Eq. (6) below mean that when $T(\varepsilon_k,\varepsilon_p,\tau,\omega)$ is evaluated, $\vec{k}$ should be replaced by $\vec{k}-\vec{q}$. To evaluate the required term of N^{-1}, we use the approximation $\nu\tau\gg1$, which has been found to be quite adequate in this case, when compared to the evaluation of T^{sp}, which does not use this approximation. In the case $\nu\tau\gg1$ we can write

$$T^*(\varepsilon_k,\varepsilon_p,\tau,\omega)=\frac{1}{(2\pi)^3}\int d^3q\left[\frac{-\mathrm{Im}\mathscr{V}_+(q,\omega)}{\pi}\right]\left[\frac{\Theta(k_F-|\vec{p}-\vec{q}|)}{|\mu|^2}-\frac{2\mathrm{P}\Theta(k_F-|\vec{p}-\vec{q}|)}{\mu\nu^*}+2\pi\delta(\nu^*)\tau\right]$$
$$\equiv\beta(\varepsilon_p,\omega)-f^*(\varepsilon_k,\varepsilon_p,\omega)+\Gamma^*(\varepsilon_k,\omega)\tau . \quad (6)$$

Here, P means that, when integrating, the Cauchy principal value is to be taken.

We now proceed to the calculation of the intensity of the spectrum due to the secondary electron-hole pair creations. The final expression for the zeroth-order contribution to the intensity is

$$I_0(\varepsilon_k)=D(\varepsilon_k)4\pi mp \tag{7}$$

with

$$0<p=[2m(\varepsilon_k-\omega_0)]^{1/2}\leq k_F\ , \tag{8}$$

and the intensity to first order in the single particle interaction is given by

$$I_1^{sp}(\varepsilon_k)=D(\varepsilon_k)\int d\omega\int d^3p\,\Theta(k_F-p)\frac{1}{(2\pi)^3}\times\int d^3q\left[\frac{-\mathrm{Im}\mathscr{V}_+^{sp}(q,\omega)}{\pi}\right]\delta(\varepsilon_k+\omega-\varepsilon_p-\omega_0)\times\left[\frac{\Theta(k_F-|\vec{p}-\vec{q}|)}{|\mu|^2}-\frac{2\Theta(k_F-|\vec{p}-\vec{q}|)}{\nu^2+(\int d\omega'\Gamma^*)^2}\left[\frac{P}{\mathrm{Re}(\mu)}\nu+\pi\delta(\mathrm{Re}(\mu))\int d\omega'\Gamma^*\right]+\frac{2}{\nu^2+(\int d\omega'\Gamma^*)^2}\right]. \tag{9}$$

The terms in the square brackets correspond to the intrinsic (first term), the interference (second and third terms), and the extrinsic (last term) processes, respectively. The prefactor $D(\varepsilon_k)$ is the same as that used in the plasmon approximation and is a slowly varying function of ε_k; it will therefore be set equal to 1, as before.[30] The expression $\int d\omega'\Gamma^*$ that appears in Eq. (9) represents the finite lifetime of the photoelectron state, which may decay via plasmon or pair production. This lifetime is dominated by the plasmon process and is usually calculated in the plasmon approximation. However, in the spirit of our calculations, we retain the single-particle contribution also. This correction is used not only in the present calculation, but also to calculate a modification to the previously reported plasmon satellite.[30] Such a correction does not alter the qualitative features of the plasmon satellite.

B. With hole renormalization

It is quite easy to see, from Eq. (7), that the zeroth-order contribution to the main band of the spectrum has the parabolic shape of the valence-band density of states. The sharp cutoff at the lower end of this curve is due to the approximation that low-lying states of the valence band have infinite lifetime. In fact, due to electron-electron interactions, such states are not infinitely long lived, and no sharp features are observed in the experimental spectra. Hence, we use a renormalized hole propagator, as an appropriate way to include these interaction effects in the zeroth-order diagram. This is shown in Fig. 2(a). The renormalization is done within the RPA, at $T=0$. Then, for $n=0$, Eq. (3) becomes

$$J_0(\varepsilon_k,\tau)=\frac{(4\pi k_F^3/3)^{-1}}{N}\int d^3p\frac{1}{\pi}\frac{\Sigma_2(p,\varepsilon_k-\omega_0)}{[\varepsilon_k-\omega_0-\varepsilon_p-\Sigma_1(p,\varepsilon_k-\omega_0)]^2+[\Sigma_2(p,\varepsilon_k-\omega_0)]^2}\ , \tag{3'}$$

where the hole self-energy is[34]

$$\Sigma(p,\omega)=\Sigma_1(p,\omega)+i\Sigma_2(p,\omega)=\frac{-m}{p(2\pi)^2}\int q\,dq\int_{(p-q)^2/2m-\omega}^{(p+q)^2/2m-\omega}d\omega'\Theta(E_F-\omega-\omega')\mathrm{Im}\mathscr{V}_+(q,\omega')\ . \tag{10}$$

Here, E_F represents the Fermi energy. Our main goal in renormalizing the hole propagator is to include the finite lifetime of the hole due to electron-electron interactions (i.e., Σ_2^{-1}). Keeping this in mind, and noting that the real part of the self-energy, Σ_1, is smoothly varying in the energy range of our interest, we omit Σ_1. This eliminates any energy shifts in the spectrum due to renormalization, thus enabling us to add the resulting intensity to other contributions, where hole-lifetime effects are not as important and, therefore, not included. The zeroth-order intensity then becomes

$$I_0(\varepsilon_k)=D(\varepsilon_k)\int d^3p\,\mathscr{L}(p,\varepsilon_k-\omega_0) \tag{7'}$$

with

$$\mathscr{L}(p,\omega)=\frac{1}{\pi}\frac{\Sigma_2(p,\omega)}{(\omega-\varepsilon_p)^2+[\Sigma_2(p,\omega)]^2}\ . \tag{11}$$

The intrinsic contribution to the intensity in Eq. (9) is found to diverge at the lower end of the main band region of the spectrum, where $\varepsilon_k=\omega_0$. This divergence is most obvious in the absence of hole recoil, where we replace $|\vec{p}-\vec{q}|$ in Eq. (9) with p. Then the hole propagator $\mu^{-1}=(\omega+i\lambda)^{-1}$, with ω being the energy of the secondary electron-hole pair, takes on the values $(i\lambda)^{-1}$ to $(E_F+i\lambda)^{-1}$ with $\lambda\to 0$. It is then easily seen that the creation of secondary electron-hole pairs of infinitesimal energy, by the primary hole, has infinitely large probabili-

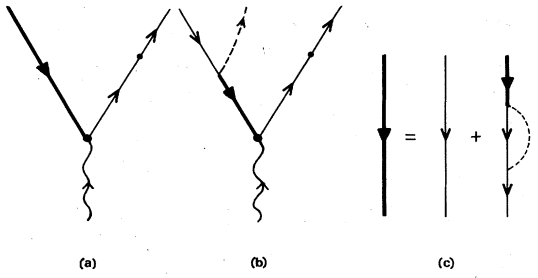

FIG. 2. Diagrams representing (a) the elastic and (b) the first-order intrinsic terms including hole renormalization. The renormalized-hole propagator is given by (c) (Dyson's equation).

ty. Such divergences have been reported previously in the calculation of x-ray emission spectra of metals.[33] As mentioned before, this is due to the approximation of infinite lifetime for all the hole states, and is not relieved by including recoil. To overcome this difficulty, it is necessary to renormalize the primary hole propagator, as shown in Fig. 2(b). We thereby include the finite lifetime of the hole, within the RPA, for calculation of the intrinsic contribution in and near the main band region of the spectrum. The net result of performing the renormalization necessary to avoid the divergence of the intrinsic term is to replace the first term in the square brackets of Eq. (9) as follows:

$$\frac{\Theta(k_F-|\vec{p}-\vec{q}|)}{|\mu|^2}$$

$$\rightarrow\left|\int_{-\infty}^{E_F}\frac{d\omega_1}{\omega+\omega_1-\varepsilon_p+i\lambda}\mathscr{L}(|\vec{p}-\vec{q}|,\omega_1)\right|^2, \quad (9')$$

with $\mathscr{L}$ defined by Eq. (11). Here, as in Eq. (7'), the real part of the hole self-energy has been dropped.

Due to the fact that the photoelectron must leave the metal before being detected, it does not become necessary to renormalize the hole propagator in the extrinsic diagram. In this contribution, the τ dependence of the electron propagator is dominant enough to avoid unphysical results due to approximations about the hole. In other words, renormalization of the hole propagator in this term will not introduce any qualitative difference in our results. The cross term between the extrinsic and the intrinsic processes, however, will be considered for renormalization.

The second quantum interference term in Eq. (9) is found to fall abruptly to zero at the lower energy end of the main band, and is zero for energies below the main band. This is due to the delta function in this term. The delta function comes directly from the infinitesimal λ when separating μ^{-1} into its real and imaginary parts. No such term is present in ν^{-1} since the photoelectron's "lifetime" is dominated by τ. In order to avoid the sharpness which would appear in the spectrum due to such a term, we renormalize the interference calculation. This is done by using the diagram of Fig. 2(b) in combination with that of Fig. 1(c) for the cross terms. For the first cross term, which will not be seriously affected by this, we take the limit of infinite lifetime, arriving at the nonrenormalized result. In the second cross term we retain the full renormalized result. The effect of the renormalization in the quantum interference is to replace factors in the third term in the square brackets of Eq. (9), as follows:

$$\Theta(k_F-|\vec{p}-\vec{q}|)\delta(\mathrm{Re}(\mu))$$

$$\rightarrow\Theta(E_F-\varepsilon_p+\omega)\mathscr{L}(|\vec{p}-\vec{q}|,\varepsilon_p-\omega) \quad (9'')$$

with $\mathscr{L}$ defined by Eq. (11).

III. CALCULATIONS AND RESULTS

Calculations have been performed for sodium, with an incoming photon energy $\omega_0=90\omega_p^0\simeq 0.5$ keV, where ω_p^0 is the plasmon energy. Each of the contributions, zeroth order, intrinsic, extrinsic, and interference, will be discussed separately.

A. Zeroth-order (elastic) term

The zeroth-order line shape is independent of ω_0 and has been computed in two approximations for comparison:

$$I_0(\varepsilon_k)=4\pi mp \quad (7'')$$

and

$$I_0(\varepsilon_k)=4\pi\int dp\,p^2\mathscr{L}(p,\varepsilon_k-\omega_0) \quad (7''')$$

with p in Eq. (7'') given by Eq. (8), $\mathscr{L}$ defined by Eq. (11), and $\varepsilon_k-\omega_0\leq E_F$. Equation (7'') uses the bare hole propagator, while Eq. (7''') has the hole renormalized as discussed. In the final analysis, the results of Eq. (7''') are retained. The results for both of the above equations are shown in Fig. 3(a).

Since electron and hole states have asymptotically infinite lifetimes as their energy approaches the Fermi energy, the two curves of Fig. 3(a) meet each other at the upper energy edge. The nonzero intensity predicted there is due to the sharpness of the Fermi surface in the present theory. Around the low-energy end of the main band region, $\varepsilon_k=\omega_0$, the larger intensities found, when hole renormalization is included, are a direct consequence of the width of the low-lying states of the conduction band in a simple metal. This allows for the smooth tailing of the main band.

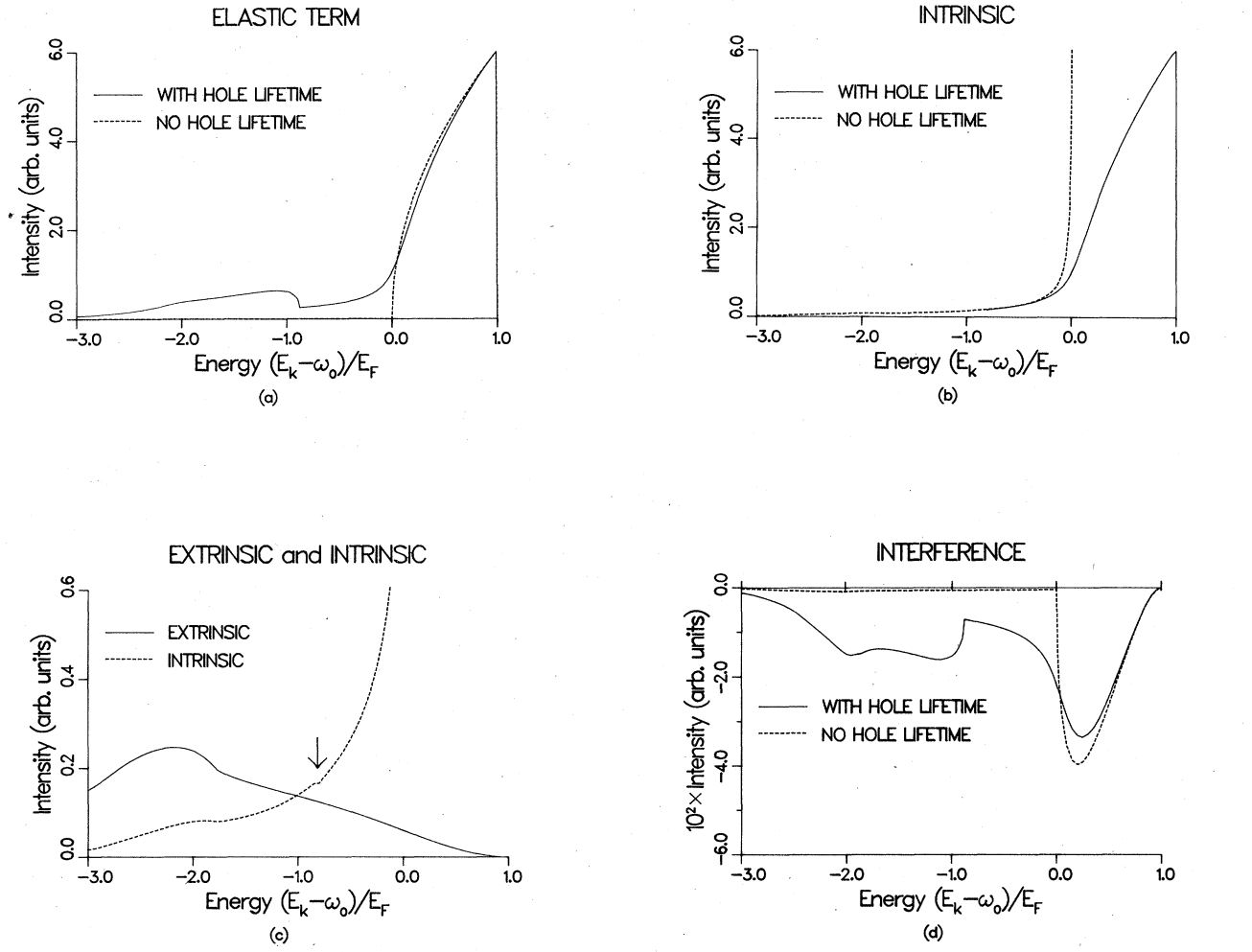

FIG. 3. The various partial intensities computed in this work: (a) elastic contribution, and (b), (c), and (d) single-particle inelastic contributions. In (c) the arrow indicates where renormalization in the intrinsic term begins (see text for details).

B. Intrinsic term

1. *Without hole renormalization*

At photoelectron energies below the main band region, conservation of energy for the overall process precludes production of secondary, single-particle excitations with vanishingly small energy. Because of this, we are able to compute the intrinsic term without including the primary hole lifetime at those energies. At photoelectron energies in the plasmon band region of the spectrum, we retain these values. This is consistent with the manner in which the plasmon contributions were computed in Ref. 30, and with other first-order terms of this calculation. In this case the intrinsic, single-particle contribution is found to be

$$I_1^{\mathrm{sp},i}(\varepsilon_k)=\frac{2m^3}{\pi^2}\int d\omega\int dq\, q[-\mathrm{Im}\mathscr{Y}_+^{\mathrm{sp}}(q,\omega)]\Theta(k_F-q+p)\times\left[\frac{1}{2m\omega-p^2+(p-q)^2}-\frac{\Theta(p+q-k_F)}{2m\omega-p^2+k_F^2}-\frac{\Theta(k_F-p-q)}{2m\omega-p^2+(p+q)^2}\right] \tag{12}$$

with

$$0<p=[2m(\varepsilon_k+\omega-\omega_0)]^{1/2}\leq k_F\ . \tag{13}$$

2. With hole renormalization

For photoelectron energies within and immediately below the main band region of the spectrum, it is necessary to include the renormalized hole propagator as previously mentioned. In this case, the contribution to the intensity in the presence of intrinsic single-particle excitations is given by

$$I_1^{\mathrm{sp},i}(\varepsilon_k)=\frac{2m^3}{\pi^2}\int d\omega\int dq\, q[-\mathrm{Im}\mathscr{Y}_+^{\mathrm{sp}}(q,\omega)] \times\frac{1}{2m^2}\int_{|p-q|}^{|p+q|} dl\, l\left[\left[\mathrm{P}\int_{-\infty}^{E_F} d\omega'\frac{\mathscr{L}(l,\omega')}{\omega'-\varepsilon_k+\omega_0}\right]^2+[\pi\mathscr{L}(l,\varepsilon_k-\omega_0)]^2\right] \tag{12'}$$

with ω restricted by Eq. (13).

The results from Eqs. (12) and (12′) are shown together in Fig. 3(b). Equation (12) is found to become quite large only for values of $\varepsilon_k-\omega_0<0.1E_F$. As the photoelectron energy approaches the plasmon band from above, the agreement between Eqs. (12) and (12′) becomes excellent, indicating that hole-lifetime effects are not important, at least down to the plasmon band, where the single-particle terms are not found to be dominant. At the upper energy edge of the main band, the small energy-transfer processes cause an interesting behavior in the renormalized theory. Here large contributions result for single-particle, intrinsic excitations. This is true since only the long-lived hole states near the Fermi surface are interacting. This contribution competes directly with the shrinking of the allowed phase space for energy transfer. Our results indicate a finite, nonzero intensity contribution at the upper energy edge of the spectrum. It is also interesting to note that the intensity of this term is of the same order of magnitude as the zeroth-order intensity throughout the main band.

C. Extrinsic term

The extrinsic contribution to the intensity, for photoemission accompanied by single electron-hole pair creation, is

$$I_1^{\mathrm{sp},e}(\varepsilon_k)=\frac{2m^2}{\pi^2 k\left[\int d\omega'\Gamma^*\right]}\int d\omega\int dq\, qp[-\mathrm{Im}\mathscr{Y}_+^{\mathrm{sp}}(q,\omega)] \times\left[\tan^{-1}\left[\frac{2m\omega-q^2+2kq}{2m\int d\omega'\Gamma^*}\right]-\tan^{-1}\left[\frac{2m\omega-q^2-2kq}{2m\int d\omega'\Gamma^*}\right]\right] \tag{14}$$

with p defined by Eq. (13). This is shown in Fig. 3(c). The maximum in this curve corresponds to strong contributions to $\mathrm{Im}\mathscr{Y}_+^{\mathrm{sp}}(q,\omega)$ from values of ω approximately equal to the cutoff plasmon energy. It is found that the extrinsic term is well behaved for all ε_k, and falls to zero at lower energies and at the upper energy edge of the main band. As discussed before, the factor $\int d\omega'\Gamma^*$ includes both the plasmon and the single-particle processes. The single-particle correction to the $\int d\omega'\Gamma^*$ of our previous calculations, using only plasmon production, amounts to 22% of the total.

D. Cross terms

1. Without hole renormalization

The contribution to the intensity from the interference between the intrinsic and extrinsic processes, in the absence of hole renormalization, is given by

$$I_1^{\mathrm{sp},x}(\varepsilon_k)=\frac{-m^3}{2\pi^2 k}\int d\omega\int dq[-\mathrm{Im}\mathscr{Y}_+^{\mathrm{sp}}(q,\omega)] \times\left\{\ln\left|\frac{(2m\omega-q^2+2kq)^2+(2m\int d\omega'\Gamma^*)^2}{(2m\omega-q^2-2kq)^2+(2m\int d\omega'\Gamma^*)^2}\right|\Theta(k_F-q+p)\right.$$

$$\times\left[\Theta(p+q-k_F)\ln\left|\frac{2m\omega-p^2+k_F^2}{2m\omega-p^2+(p-q)^2}\right|\right.$$

$$\left.\left.+\,\Theta(k_F-p-q)\ln\left|\frac{2m\omega-p^2+(p+q)^2}{2m\omega-p^2+(p-q)^2}\right|\right]\right\}$$

$$+2\pi\Theta(2pq-q^2-2m\omega)\left[\tan^{-1}\left[\frac{2m\omega+2kq-q^2}{2m\int d\omega'\Gamma^*}\right]\right.$$

$$\left.-\tan^{-1}\left[\frac{2m\omega-2kq-q^2}{2m\int d\omega'\Gamma^*}\right]\right]\Bigg\} \tag{15}$$

with p defined by Eq. (13). The log terms are well behaved for all ε_k, and approach zero where expected, but are much smaller than the $\tan^{-1}$ terms. The contribution from these latter, dominant, terms falls abruptly to zero at the lower end of the main band region. The total contribution from all terms in Eq. (15) is shown as the dashed line in Fig. 3(d).

2. *With hole renormalization*

In order to find the spectrum under the more realistic condition of finite hole lifetime, the quantum interference was renormalized, as explained in the preceding section. Since only the dominant cross term of Eq. (9) is significantly affected by hole lifetime, it is the only one for which hole-lifetime effects were included. The resulting expression is

$$I_1^{\mathrm{sp},x}(\varepsilon_k)=\frac{-m^3}{2\pi^2 k}\int d\omega\int dq[-\mathrm{Im}\mathscr{Y}_+^{\mathrm{sp}}(q,\omega)]$$

$$\times\Bigg\{\ln\left|\frac{(2m\omega-q^2+2kq)^2+(2m\int d\omega'\Gamma^*)^2}{(2m\omega-q^2-2kq)^2+(2m\int d\omega'\Gamma^*)^2}\right|\Theta(k_F-q+p)$$

$$\times\Bigg[\Theta(p+q-k_F)\ln\left|\frac{2m\omega-p^2+k_F^2}{2m\omega-p^2+(p-q)^2}\right|$$

$$+\Theta(k_F-p-q)\ln\left|\frac{2m\omega-p^2+(p+q)^2}{2m\omega-p^2+(p-q)^2}\right|\Bigg]$$

$$+\frac{2\pi}{m}\Theta(E_F-\varepsilon_k+\omega_0)\left[\tan^{-1}\left[\frac{2m\omega+2kq-q^2}{2m\int d\omega'\Gamma^*}\right]-\tan^{-1}\left[\frac{2m\omega-2kq-q^2}{2m\int d\omega'\Gamma^*}\right]\right]$$

$$\times\int_{|p-q|}^{p+q} dl\, l\mathscr{L}(l,\varepsilon_k-\omega_0)\Bigg\}. \tag{15'}$$

Its contribution is shown by the solid line in Fig. 3(d).

An examination of the two curves of Fig. 3(d) shows the effect of renormalization on the cross term to be similar to that in the zeroth-order case. In addition to tailing of the main band intensities, there is an increase in magnitude at plasmon band energies due to virtual plasmon processes included by the renormalization. Overall, the cross terms in the single-particle case are not found to be as important as in the plasmon case, at this photoelectron energy. In the final analysis only the results of Eq. (15′) are retained.

E. Total valence-band spectrum

The total intensity of the valence-band photoemission spectrum was obtained by adding together the renormalized zeroth-order (elastic) contribution, the single-particle excitation terms and the results due to plasmon excitation from Ref. 30. The result is shown in Fig. 4. As mentioned before, the plasmon values were adjusted by including the appropriate photoelectron lifetime, calculated by using both plasmon and single-particle effects. The single-particle, intrinsic contribution in Fig. 4 is calculat-

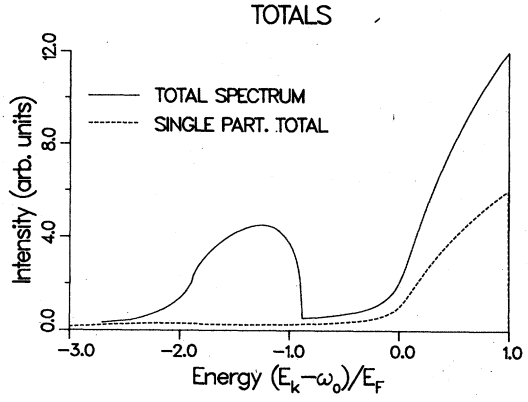

FIG. 4. The total single-particle contribution (dashed line) and the total spectrum including elastic and inelastic scattering effects for bulk processes (solid line).

ed including hole lifetime effects at photoelectron energies above the plasmon band, and the renormalized results for the quantum interference are used over the entire spectral range.

IV. SUMMARY AND CONCLUSIONS

The primary concern of this work has been to include the effects of the production of single, secondary electron-hole pairs on valence-band XPS. We have computed both the shape and magnitude of the valence-band x-ray photoemission spectrum for sodium metal. The results of this study are combined with those of a previous work,[30] and the net result, including the main band and the first plasmon satellite regions, is shown in Fig. 4.

We have found, in the main band region of the spectrum, that the intrinsic contribution involving single-particle processes diverges in the first-order theory. Such divergences in the first-order theory are not unusual and, in fact, have been found in the calculations of the soft x-ray emission spectra[31,33] and the valence-band Auger spectra of metals.[32] However, in the tailing region of the main band, and at lower energies, this first-order intrinsic intensity is finite, and is of the same order of magnitude as the well-behaved extrinsic contribution. The quantum interference for the single-particle process considered is found to be, generally, much smaller than the intrinsic and the extrinsic intensities. The first-order theory has a weak maximum in the plasmon satellite tail due to near-resonant behavior of the single-particle excitations around the plasmon cutoff frequency.

In order to avoid the divergence in the first-order intrinsic term in the main band region and to eliminate the sharp cutoff of the parabolic zeroth-order intensity and of the cross term, it is necessary to include the virtual, intrinsic pair productions to all orders, that is, to renormalize the primary hole propagator. This corresponds to including the finite lifetime of the primary hole, which controls the intrinsic process. The inclusion of primary hole lifetime results in a smooth, finite spectrum. The shape and magnitude of the single-particle, intrinsic contribution closely follows that of the renormalized, no loss intensity in the main band. This is evidence that a major process here is the production, by the primary hole, of small energy electron-hole pairs. The process, however, is limited by the finite lifetime of the primary hole. Since the primary electron (photoelectron) is created with large energy, its lifetime is long and is really dominated by the detection process.

The calculated valence-band photoemission spectrum of sodium, as shown in Fig. 4, is smooth and finite over the entire spectral range. The main (no-loss) band is separated from the first plasmon satellite band by a smooth tail. The main band retains its parabolic shape, even though it is significantly enhanced by the single-particle processes. The plasmon satellite is relatively wider than the main band due to the inclusion of the dispersion of the plasmon frequency and is somewhat enhanced by the renormalization of the no-loss diagram. We find the ratio of the integrated intensity in the plasmon band region to that above the satellite to be 54%.

It is interesting to attempt to compare our results with the currently available experimental spectra for sodium.[22,25] Such a comparison is shown in Fig. 5. The points represent the raw data taken from Fig. 3 of Ref. 25(b), with the minimum recorded intensity subtracted from all points. The solid line is the final result of our theory convoluted with a 0.6-eV Gaussian spectrometer resolution function. Peak intensities were matched, and the abscissas were adjusted using the free-electron value of E_F. It must be noted, though, that the theoretical results do not include the effect of surface plasmon production,

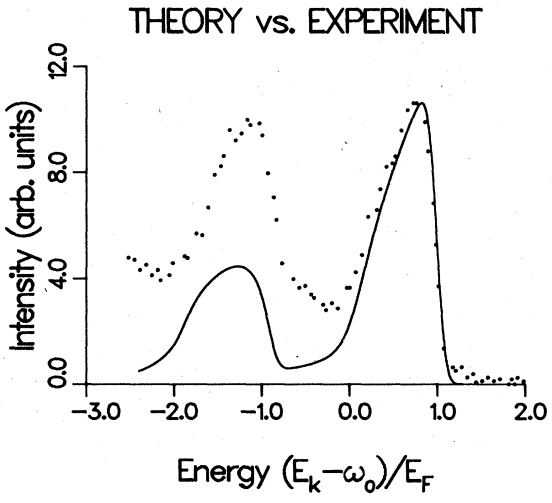

FIG. 5. Comparison of theory convoluted with 0.6-eV Gaussian resolution function (solid line), and experimental data taken from Fig. 3 of Ref. 25 (b) (points).

which increase the intensity between the main band and the bulk plasmon satellite. In addition to this, a quantitative difference is expected due to inelastic scattering from impurities, phonons, and crystal boundaries. Although our calculations do include inelastic scattering between electrons, they do not include these nonideal scatterings which give rise to the inelastic background. However, the effect of such processes is to shift intensity from the main band to lower spectral energies, thereby increasing the peak intensity of the plasmon satellite relative to the main band, as is found. With this in mind, we see qualitative agreement between our present results and the experimental data.

In summary, we would like to emphasize that in this paper, we have presented the first *ab initio* calculation of the valence-band photoemission spectrum of a simple metal, which includes the important electron-electron interaction effects (including intrinsic, extrinsic, and interference terms) that introduce significant contributions to the spectrum. We have obtained results for the main band and the first plasmon satellite, which qualitatively agree with the presently available experimental spectra.

ACKNOWLEDGMENT

The authors would like to thank Dr. P. Longe for many helpful discussions.

---

*Based in part on a thesis submitted by S. Prutzer in partial fulfillment of the requirements for the degree of Doctor of Philosophy at Drexel University, June, 1984.

†Present address: General Electric Company, 3198 Chestnut Street, Philadelphia, Pennsylvania 19101.

[1]For reviews, see P. Steiner, H. Höchst, and S. Hüfner, in *Topics in Applied Physics,* edited by L. Ley and M. Cardona (Springer, Berlin, 1979), Vol. 27, p. 349; J. W. Gadzuk, in *Photoemission and the Electronic Properties of Surfaces,* edited by B. Feuerbacher, B. Fitton, and R. F. Willis (Wiley-Interscience, New York, 1978), p. 111.

[2]S. Doniach and M. Šunjić, J. Phys. C **3**, 285 (1970).

[3]D. C. Langreth, Phys. Rev. B **1**, 471 (1970).

[4]S. M. Bose, P. Kiehm, and P. Longe, Phys. Rev. B **23**, 712 (1981).

[5]B. I. Lundqvist, Phys. Kondens. Mater. **9**, 236 (1969).

[6]J. J. Chang and D. C. Langreth, Phys. Rev. B **8**, 4638 (1973); D. C. Langreth, in *Collective Properties of Physical Systems, 24th Nobel Symposium,* edited by B. I. Lundqvist and S. Lundqvist (Academic, New York, 1974), p. 210.

[7]M. Šunjić and D. Šokčević, Solid State Commun. **15**, 165 (1974); **18**, 373 (1976); M. Šunjić, D. Šokčević, and A. Lucas, J. Electron Spectrosc. Relat. Phenom. **5**, 963 (1974).

[8]D. R. Penn, Phys. Rev. Lett. **38**, 1429 (1977).

[9]D. Chastenet and P. Longe, Phys. Rev. Lett. **44**, 91 (1980); **44**, 903(E) (1980).

[10]J. E. Inglesfield, Solid State Commun. **40**, 467 (1981); J. Phys. C **16**, 403 (1983).

[11]S. M. Bose, S. Prutzer, and P. Longe, Phys. Rev. B **27**, 5992 (1983).

[12]P. Longe, P. Kiehm, and S. M. Bose, Phys. Rev. B **27**, 6000 (1983).

[13]W. J. Pardee, G. D. Mahan, D. E. Eastman, R. A. Pollak, L. Ley, F. R. McFeely, S. P. Kowalczyk, and D. A. Shirley, Phys. Rev. B **11**, 3614 (1975).

[14]J. C. Fuggle, D. J. Fabian, and L. M. Watson, J. Electron Spectrosc. Relat. Phenom. **9**, 99 (1976).

[15]R. S. Williams, P. S. Wehner, G. Apai, J. Stöhr, D. A. Shirley, and S. P. Kowalczyk, J. Electron Spectrosc. Relat. Phenom. **12**, 477 (1977).

[16]S. A. Flodstrom, R. Z. Bachrach, R. S. Bauer, J. C. McMenamin, and S. B. M. Hagström, J. Vac. Sci. Technol. **14**, 303 (1977).

[17]P. H. Citrin, G. K. Wertheim, and Y. Baer, Phys. Rev. B **16**, 4256 (1977).

[18]D. Norman and D. P. Woodruff, Surf. Sci. **79**, 76 (1979).

[19]L. I. Johansson and I. Lindau, Solid State Commun. **29**, 379 (1979).

[20]P. Steiner, H. Höchst, and S. Hüfner, Z. Phys. B **30**, 129 (1978).

[21]Y. Baer and G. Busch, Phys. Rev. Lett. **30**, 280 (1973).

[22]S. P. Kowalczyk, L. Ley, F. R. McFeely, R. A. Pollak, and D. A. Shirley, Phys. Rev. B **8**, 3583 (1973).

[23]P. H. Citrin, Phys. Rev. B **8**, 5545 (1973).

[24]P. M. Th. M. Van Attekum and J. M. Trooster, Phys. Rev. B **18**, 3872 (1978).

[25](a) H. Höchst, P. Steiner, and S. Hüfner, J. Phys. F **7**, L309 (1977); (b) Z. Phys. B **30**, 145 (1978).

[26]S. Doniach, Phys. Rev. B **2**, 3898 (1970).

[27]D. R. Penn, Phys. Rev. Lett. **40**, 568 (1978).

[28]L. Hedin, Phys. Scr. **21**, 477 (1980).

[29]P. Longe and S. M. Bose, Solid State Commun. **38**, 527 (1981).

[30]S. M. Bose, S. Prutzer, and P. Longe, Phys. Rev. B **26**, 729 (1982).

[31]S. M. Bose and A. J. Glick, Phys. Rev. B **10**, 2733 (1974).

[32]J. Fitchek, R. Patrick, and S. M. Bose, Phys. Rev. B **26**, 6390 (1982).

[33]P. Longe and A. J. Glick, Phys. Rev. **177**, 526 (1969).

[34]S. M. Bose, A. Bardasis, A. J. Glick, D. Hone, and P. Longe, Phys. Rev. **155**, 379 (1967).